Detection of Conformation Change in Specific Residue for α-synuclein (61-95) in Monolayer

By

Damilola Ogunmola

A Thesis Submitted in Partial Fulfillment of the Requirements for the Degree of

Master of Science in Chemistry

Middle Tennessee State University

September 2024

Thesis Committee:

Dr. Chengshan Wang, Chair

Dr. Keying Ding

Dr. Souvik Banerjee

In the loving memory of my parents, Segun and Bimpe, forever in my heart.

ABSTRACT

Membrane proteins cause challenges for the major techniques (i.e., X-ray crystallography, NMR, and cryo-Electron Microscopy) to determine protein's structure with high resolution. For example, it is difficult for membrane proteins to form single crystal structure required by X-ray. For NMR, the tumbling rate will be decreased substantially for membrane proteins. As a recent developed technique, cryo-Electron Microscopy (cryo-EM) requires mono-dispersed and unified samples in frozen state. Therefore, coexisting conformations in residues in protein's structure are not welcome. In addition, all the techniques above cannot provide high resolution results for monolayer structure, which is the native state of membrane proteins. α-Synuclein (α-syn) is a membrane protein with 140 amino acids in the sequence and its abnormal aggregation is related to Parkinson's disease (PD). In the sequence of α-syn, the non-amyloid component (NAC) spanning residues 61 to 95 is critical for the aggregation. In this thesis, p-polarized Multiple Incidence Angle Resolution Spectrometry (pMAIRS) was used to examine the NAC monolayer formed at interface. After two hours compression, coexisting conformation (i.e., the transition stage of the conformation change) was detected at residue 68G in NAC by pMAIRS. With residue level resolution for coexisting conformations, pMAIRS power for monolayers was exhibited. Furthermore, 68G was found to completely change its conformation from α-helix to β-sheet after three days compression. To our best knowledge, this is the first report to detect the conformation change of a specific residue in a peptide in monolayer structure. Therefore, pMAIRS can supplement the major techniques mentioned above to address protein's (especially membrane proteins) structure.

ACKNOWLEDGEMENTS

My gratitude goes to my research advisor Dr. Chengshan Wang for his guidance and invaluable assistance in my thesis research. Always available to listen and help with my utmost interest at heart, I am immensely grateful.

Additionally, I would like to express my gratitude to Dr. Keying Ding and Dr Souvik Banerjee from my thesis committee for their time spent examining my thesis and offering insightful criticism of my work.

I would especially like to express my gratitude to the MTSU College of Graduate Studies and the College of Basic and Applied Sciences for supporting and providing programs that allow students such as myself to share and present our research. The chemistry department at MTSU has been a great help in advancing my professional objectives by offering tools to support my chemical research.

Also, I want to thank Jessie Weatherly for his assistance with troubleshooting and fixing the instrument when we had a breakdown. I would Tayo and Toyin who are members of Dr Wang's lab for the team work efforts, time and sacrifices towards the success of the group.

TABLE OF CONTENTS

LIST OF FIGURES vi

LIST OF TABLE AND EQUATIONS ix

CHAPTER 1 1

INTRODUCTION 1

1.1 Amino acids, Protein, and Membrane Protein 1

1.2 Problems of Membrane Proteins for Methodology for Protein Structure. 3

1.3 FTIR Spectroscopy for Proteins and Surface FTIR. 4

1.4 α-synuclein (α-syn) and α-syn(61-95) segments. 6

1.5 Surface Chemistry and Spectroscopy of α-Syn(61-95) at Air-Water Interface. 7

1.6 13C Isotope Edited FTIR and pMAIRS 11

1.7 Thesis Motivation. 14

CHAPTER 2 17

METHOD AND MATERIALS 17

2.1 Peptide Synthesis 17

2.3 Mass Spectroscopy 21

2.3.1 Mass Spectroscopy using Waters Synapt Tandem Mass spectrometer 21

2.3.2 Mass Spectroscopy Bruker Compact QTOF 22

2.4 Langmuir Monolayer Technique. 23

2.5 p-Polarized Multiple Angle Incidence Resolution Spectroscopy (pMAIRS) 23

CHAPTER 3 25

RESULTS AND DISCUSSIONS 25

3.1 Orientation May Cause the Decreasing Molecular Area. 25

3.2 Mass Spectroscopy of ^{13}C Labeled α-Syn(61－95) at 68G 28

3.3 Conformation Change was Detected by the pMAIRS of the Monolayer of ^{13}C Labeled α-syn(61－95) at 68G. 30

3.4 Results of Monolayer Compressed with Extensive Time 34

3.5 Discussions 37

3.6 Conclusion 40

REFERENCES 41

LIST OF FIGURES

Figure 1.1. The illustration about the orientation of (A) α-helix on supported phospholipid bilayer (SPB) and (B) β-sheet strand perpendicular to the SPB (middle) and the enlargement of a typical residue with both the C=O and C_α–H parallel to the surface of SPB (right)……..…….....6

Figure 1.2. The sequence of α-syn with the N-terminus expressed in Italics and the C-terminus underlined……..……..……....7

Figure 1.3. Surface pressure-area isotherm of α-syn(61－95) on: pure water (solid line) and 0.5 M NaCl (dashed line)…….……...……....8

Figure 1-4. CD spectra of α-syn Langmuir-Blodgett film on quartz slides (solid line curve) under 6 mN/m and 0.075 mg/mL α-syn(61－95) dissolved in pure water (dashed line curve), respectively……..9

Figure 1-5. p-MAIRS results of the LB film of α-syn(61－95) transferred under 6 mN/m….10

Figure 1.6. Illustration of two probabilities of α-syn(61-95) at the air-water interface……...11

Figure 1.7. pMAIRS results of the LB monolayer of the ^{13}C labeled α-syn(61-95) at position 93G……..…13

Figure 1.8. Stability curves when the Langmuir monolayer of α-syn(61－95) was compressed up to 6mN/m and kept constant for more than two hours on pure water subphase. Solid curve is for surface pressure and dashed curve is for molecular area……..…15

Figure 2.1. CEM microwave peptide synthesizer……..…18

Figure 2.2. Overview of solid phase peptide synthesis…….…….19

Figure 2.3. Waters Breeze 2 separation system…….20

Figure 2.4. Waters synaptic tandem mass spectrometer……21

Figure 2.5 Compact QTOF (Compass 1.9, otofControl 4.0) interfaced with an electrospray ionization

(ESI)……...22

Figure 2.6. Kibron μ-trough XS……..23

Figure 2.7. Thermo Fischer Nicolet iS50R FTIR with electronic rotary stage component…..……24

Figure 3.1. Illustration for small amphiphilic lipid molecules orient more perpendicular to the interface during the compression……25

Figure 3.2. pMAIRS results of the LB monolayer of unlabeled α-syn(61－95) transferred after the surface pressure was held at 6 mN/m for two hours……....26

Figure 3.3. Mass spectroscopy from Waters q-TOF spectrometer……..…28

Figure 3.4. Mass spectroscopy from Bruker q-TOF spectrometer…….....29

Figure 3.5. The zoom-in of the peak at 1652.44 Da……30

Figure 3.6. p-MAIRS results of the LB monolayer of ^{13}C labeled α-syn(61－95) at 68G transferred after the surface pressure was held at 6 mN/m for 15 minutes…….32

Figure 3.7. p-MAIRS results of the LB monolayer of ^{13}C labeled α-syn(61－95) at 68G transferred after the surface pressure was held at 6 mN/m for 2 hours……33

Figure 3.8. Usual Langmuir monolayer trough without the cover…….....34

Figure 3.9. Langmuir monolayer trough with the cover……...…..35

Figure 3.10. p-MAIRS results of the LB monolayer of ^{13}C labeled α-syn(61－95) at 68G

transferred after the surface pressure was held at 6 mN/m for 3 days……..36

Figure 3.11. Conformation changes with intermolecular hydrogen bond formation during the compression of α-syn(61－95) at interface……..39

LIST OF TABLE AND EQUATIONS

Table 1: Amino acids and their respective R groups……2

Equation 1……5

CHAPTER 1

INTRODUCTION

1.1 Amino acids, Protein, and Membrane Protein

The biochemical processes *in vivo* are facilitated and accomplished by proteins and therefore the determination of the protein's structure is an important topic in biochemistry.[1-3] . Proteins in human biological systems are comprised of 20 naturally occurring amino acids. Amino acids are comprised of an amino group, a carboxyl group, a R group and hydrogen atom all bonded to an alpha carbon. The R group which is directly attached to the alpha carbon is the distinguishing factor among the different amino acids (**Table 1**). Proteins are formed from extended chains of amino acids joined by amide bond, which is a covalent bond that is formed when the carboxyl (-COOH) group of one amino acid combines with the amino ($-NH_2$) group of neighboring amino acid.[4] Peptides are smaller units of linked amino acids. Both peptides and proteins can fold into precise three-dimensional forms that are essential to their biological activities.

As for protein's structure, the order of the amino acids in a protein is known as its primary structure. The primary structure in turn forms the secondary structure, which is the specific geometric shape caused by inter and intra-molecular hydrogen bonding in the amide groups. The secondary structure is usually referred to as the conformation of the protein and it includes three major forms, α-helix, β sheets, and random coils. The final structure and function of the protein are determined when the secondary structure elements pack tightly to 3D structures and it is called the tertiary structure of the protein.

Proteins found in and around the vesicles are usually referred to as membrane protein and alpha synuclein is one of such proteins.[6] Membrane proteins are involved in endogenous as well as exogenous procedures and malfunction of membrane proteins will cause various diseases.[4-8]

Consequently, it is also important to determine the structure of membrane proteins. However, membrane proteins cause challenges for major techniques to address protein's structure.

Table 1: Amino acids and their respective R groups

Amino acid	Abbreviations/Alphabet Notation		Structure of R group
Alanine	Ala	A	$-CH_3$
Arginine	Arg	R	$-(CH_2)_3-NH-C(NH_2)=NH$
Asparagine	Asn	N	$-CH_2-CO-NH_2$
Aspartic acid	Asp	D	$-CH_2-COOH$
Cysteine	Cys	C	$-CH_2-SH$
Glutamine	Gln	Q	$-(CH_2)_2-CO-NH_2$
Glutamic Acid	Glu	E	$-(CH_2)_2-COOH$
Glycine	Gly	G	-H
Histidine	His	H	-CH2C3H3N2
Isoleucine	Ile	I	$-CH(CH_3)-CH_2-CH_3$
Leucine	Leu	L	$-CH_2-CH-(CH_3)_2$
Lysine	Lys	K	$-(CH_2)_4NH_2$
Methionine	Met	M	$-(CH_2)_2-S-CH_3$
Phenylalanine	Phe	F	$-CH_2-C_6H_5$
Proline	Pro	P	$-CH(CH_2)_3NH$
Serine	Ser	S	$-CH_2-OH$
Threonine	Thr	T	$-CH(OH)-CH_3$
Tryptophan	Trp	W	$-CH_2-C_8H_6N$
Tyrosine	Tyr	Y	$-CH_2-C_6H_5-OH$
Valine	Val	V	$-CH-(CH_3)_2$

1.2 Problems of Membrane Proteins for Methodology for Protein Structure.

For example, X-ray crystallography is a powerful technique to determine the three-dimensional (3D) structure of proteins/peptides at the atomic level.[3, 9, 10] However, lots of membrane proteins cannot form single crystal required by X-ray crystallography. As for NMR, membrane proteins containing repeating sequences caused serious overlapped signal.[6] In addition, membrane proteins usually reside around cell membrane composed of a phospholipids bilayer structure, which decreases the tumbling rates of NMR.[6] As a recent developed powerful technique, cryo-Electron Microscopy (cryo-EM) attracted more and more attention for the determination of membrane proteins/peptides structure.[4, 7] Sample for Cryo-EM is usually loaded to cryo-grids which comprises a metal support mesh on a holey carbon film for a well dispersed and unified proteins/peptides samples.[11] It is not a surprise that proteins with equilibrating conformations during conformation change are not welcome by cryo-EM.[12]

It is worth noting that membrane proteins usually form monolayer structure around cell membranes and vesicles.[12, 13] In the monolayer, membrane proteins either lay parallel to the surface of membrane or form transmembrane structures.[12, 13] Notice that all of the three major techniques are for bulky proteins samples. In other words, none of them can provide high resolution results for proteins in monolayer structure, which is the native state of membrane proteins. Therefore, surface techniques have been developed to address this issue. For example, Atomic Force Microscopy (AFM) has been used to study the morphology of monolayer and small angle X-ray diffraction as well as ellipsometry has been utilized to evaluate the thickness of monolayer.[14, 15] In addition, the air-water interface shows similar amphiphilic character to cell membranes and can be combined with surface spectroscopic techniques to study membrane protein's structure in monolayer.[16, 17] Among various techniques, FTIR is an important one as described below.

1.3 FTIR Spectroscopy for Proteins and Surface FTIR.

FTIR spectroscopy is also an important technique to evaluate the major secondary structure in a peptide/protein.[18] This is achieved by the characteristic peak position of amide I band (from 1600 to 1700 cm^{-1}), which mainly stems from the stretching mode vibration of the backbone carbonyls (i.e., C=O). For example, the amide I band of α-helix is around 1650 cm^{-1}, whereas that of β-sheet is at 1630 cm^{-1}, and that of the unstructured conformation is at 1640 cm^{-1}.[18] By deconvoluting the amide I band, the major conformation in a peptide/protein can be evaluated.[18, 19] Together with supported phospholipids bilayer (SPB) structure mimicking cell membrane,[13, 20] surface FTIR techniques have been used to evaluate the orientation of membrane peptides/proteins at the interface.[18, 21, 22] The major surface FTIR techniques, namely, Infrared External Reflection Spectroscopy (IR-ERS), Attenuated Total Reflection (ATR), and p-polarized Multiple Angle Incidence Resolution Spectroscopy (pMAIRS).

pMAIRS shows novel advantage when compared with early developed surface FT-IR techniques, such as ATR technique and IR-ERS.[15] For example, ATR requires high refractive index substrates which are limited, whereas pMAIRS can be applied on much more substrates (e.g., CaF_2).[15] As for IR-ERS, p-polarized IR beam is used to irradiate and the reflection is used to determine the orientation of transition moments. The reflection of p-polarized IR beam around magic angle (i.e., 53.5) is almost zero and consequently, the quantitative evaluation about tilted angle of transition moments around magic angle is difficult for IR-ERS.[15] In addition, quantitative evaluation about tilted angle of a transition moment by IR-ERS requires both experimental measurement and theoretical calculations. All of the above mentioned requirement challenges lots of researchers to employ IR-ERS.[15] On the contrary, the measurements of pMAIRS are straight

forward and the results are decomposed to in-plane (IP) spectrum and out-of-plane (OP) spectrum automatically after the measurement. The IP results contain all the transition moments parallel to the surface of the substrate and the OP contains the perpendicular ones. The tilted angle 90-ϕ of a transition moment can be quantitatively evaluated by Equation 1 below. A_{IP} and A_{OP} are the peak intensity of a vibration in IP and OP results, respectively.[23, 24] The tilted angle/orientation of various conformations or secondary structures in a peptide/protein can also be accurately determined as shown below in **Figure 1.1**.

$$\phi = \tan^{-1}\sqrt{\frac{2A_{IP}}{A_{OP}}} \qquad \text{Equation (1)}$$

In α-helix, the vibration of the stretching mode of the backbone C=O is roughly parallel to the direction of the axis of α-helix as shown in **Figure 1.1A**.[25] Therefore, the orientation of the axis of α-helix can be determined by the amide I band in pMAIRS. As for the strand in β-sheet conformation, the orientation of the strand is perpendicular to both the backbone C=O and the C_α–H as shown in **Figure 1.1B**. Thus, the orientation of the strand in in β-sheet conformation can be also accurately evaluated by the amide I band and the C_α–H in pMAIRS.[26] For example, both the backbone C=O and C_α–H will be parallel to the surface of SPB if the strand in β-sheet conformation is perpendicular to the surface as shown in **Figure 1.1B**.[26] Therefore, we have utilized surface FTIR to analyze α-synuclein (α-syn) and its segment peptide.[23, 24, 27] The next section will introduce the background of α-syn and its segment peptide.

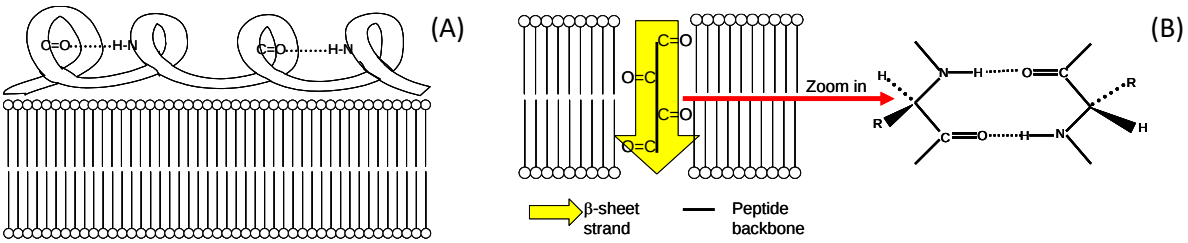

Figure 1.1. The illustration about the orientation of (A) α-helix on supported phospholipid bilayer (SPB) and (B) β-sheet strand perpendicular to the SPB (middle) and the enlargement of a typical residue with both the C=O and C_α–H parallel to the surface of SPB (right).

1.4 α-synuclein (α-syn) and α-syn(61-95) segments.

α-Syn is a 140-amino-acid protein (sequence shown in **Figure 1.2**)[28, 29] accumulating in presynaptic terminals where exist high concentration of membrane structure such as vesicles.[19, 30] Although the function is still not known, α-syn is the major protein component in Lewy bodies which are the abnormal hallmark aggregates in the brain of Parkinson's disease (PD) patients.[28, 29] It is worth noting that segment peptides of α-syn are also present in Lewy bodies. The sequence of α-syn has been divided into three regions, namely, N-terminus (residues 1-60), C-terminus (residues 96-140), and non-amyloid component (residues 61-95).[31] Although the name is non-amyloid component (termed as α-syn(61-95) here after), α-syn(61-95) is highly prone to aggregation and has been also detected in Lewy bodies together with the α-syn whole protein.[32] In addition, α-syn(61-95) has been detected in the senile plaques together with the β-amyloid peptide

in the brain of Alzheimer's disease (AD) patients.[33]

MDVFMKGLSK AKEGVVAAAE KTKQGVAEAA GKTKEGVLYV GSKTKEGVVH GVATVAEKTK EQVTNVGGAV VTGVTAVAQK TVEGAGSIAA ATGFVKKDQL GKNEEGAPQE GILEDMPVDP DNEAYEMPSE EGYQDYEPEA

Figure 1.2. The sequence of α-syn with the N-terminus expressed in Italics and the NAC region underlined.

Despite its high relevance with both AD and PD, biophysical and biochemical study of α-syn(61-95) has been overlooked for a long time. Thus, our group started to study the surface chemistry of α-syn(61-95) by air-water interface,[16, 17, 23, 24, 27] which shows similar properties to the amphiphilic natures (such as vesicles and cell membranes) with high concentration existing in the presynaptic terminals.[31, 34] α-Syn(61-95) was found to be unstructured in aqueous solution and form a monolayer at the air-water interface.[23] More importantly, surface FT-IR was also used to examine α-syn(61-95) in monolayer structure as below.

1.5 Surface Chemistry and Spectroscopy of α-Syn(61-95) at Air-Water Interface.

Figure 1.3 shows the surface pressure-area (π－A) isotherm of α-syn(61－95). When the subphase was pure water, the lift-off point of the π－A isotherm was at 400 $Å^2$/molecule,

followed by a steady increase of the surface pressure up to a kink point at 360 Å^2/molecule. Decreasing the surface area further caused the surface pressure to increase quickly and the collapse was observed at 205 Å^2/molecule with a surface pressure at 17 mN/m. The limiting molecular area was obtained at 350 Å^2/molecule by extrapolating the higher surface pressures of the isotherm to nil surface pressure. When high concentration of NaCl (0.5 M) was added into the subphase, the limiting molecular area does not increase much (cf, the dashed line in **Figure 1.3)**. This means that the amphiphilic nature of the interface is the major reason to keep α-syn(61－95) at the interface. Then a question arises: why α-syn(61－95) is kept at the interface? This question is interesting because α-syn(61－95) is unstructured in aqueous solution and the unstructured conformation does not show the preference to stay at the interface. To address this question, a Langmuir monolayer of α-syn(61－95) was transferred onto quartz slides as Langmuir-Blodgett (LB) film and Circular Dichroism (CD) spectra of both the aqueous solution of α-syn(61－95) and the LB film are shown in **Figure 1.4**.

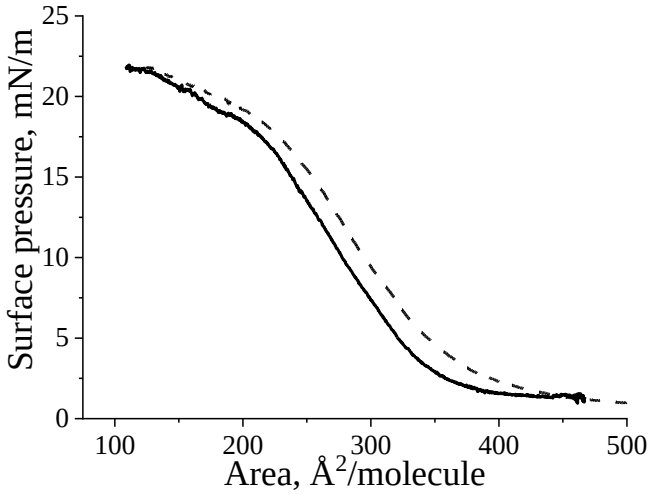

Figure 1.3. Surface pressure-area isotherm of α-syn(61－95) on: pure water (solid line) and 0.5 M NaCl (dashed line). Adapted from reference with permission[23].

For the α-syn(61－95) in aqueous solution, only one negative peak is detected at 199 nm, which is assigned to unstructured conformation.[27] As for the LB film of α-syn(61－95) on quartz slides, two negative peaks were detected at 208 & 221 nm together with another positive peak at 191 nm.[27] All the peaks above are the characteristic of α-helix and therefore, α-syn(61－95) transforms to α-helix in the LB film. To ensure the α-helical conformation of the α-syn(61－95) at the interface and determine the tilt angle of the axis of α-helix to the interface, the Langmuir monolayer of α-syn(61－95) was transferred onto a silicon substrate under 6 mN/m and examined by pMAIRS.

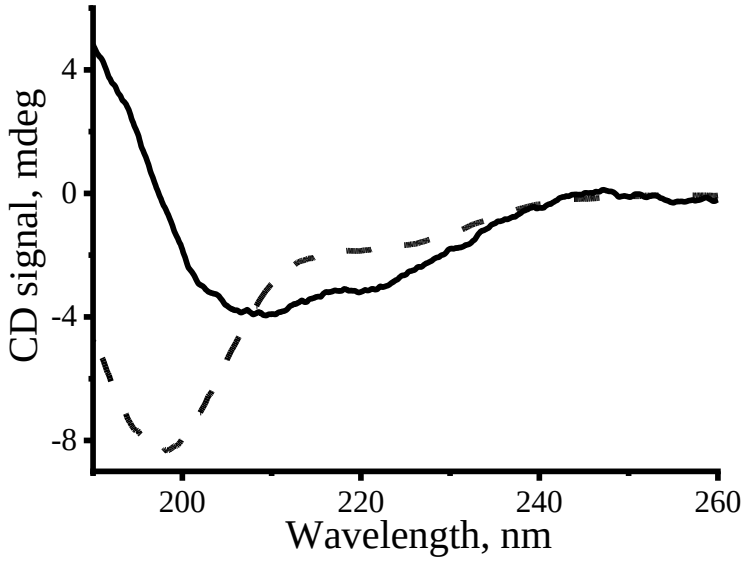

Figure 1.4. CD spectra of α-syn Langmuir-Blodgett film on quartz slides (solid line curve) under 6 mN/m and 0.075 mg/mL α-syn(61－95) dissolved in pure water (dashed line curve), respectively. Adapted from reference with permission[23-24].

As shown in **Figure 1.5**, the amide I band at 1658 cm^{-1}, which is the characteristic peak of α-helix, was detected in both the S_{IP} and S_{OP} in the pMAIRS spectra of α-syn(61-95).[23] Together with the circular dichroism (CD) spectroscopy, α-syn(61-95) was found to transform to α-helix at the interface. In addition, the tilted angle of the axis of α-helical α-syn(61-95) was examined by p-polarized Multiple-Angle Incidence Resolution Spectrometry (pMAIRS) by Equation 1 mentioned above.[23, 24] Roughly, the peak intensity of the amide I band at 1658 cm^{-1} in S_{IP} and S_{OP} in **Figure 1.5** is used to evaluate the tilt angle of the amide I transition moment to be 30.1 º.

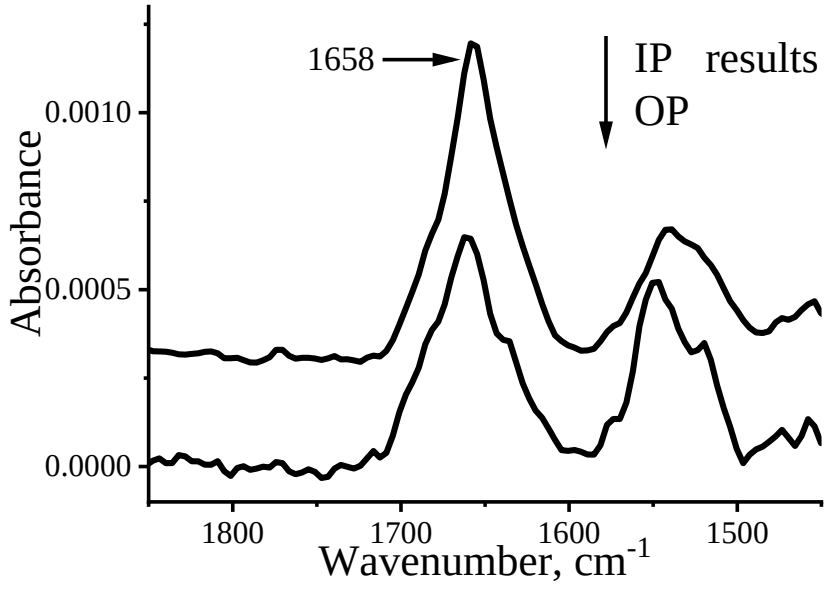

Figure 1-5. p-MAIRS results of the LB film of α-syn(61－95) transferred under 6 mN/m.

Adapted from reference with permission[23]

1.6 13C Isotope Edited FTIR and pMAIRS

It is worth noting that the traditional FT-IR technique can only provide "low-resolution" results, which cannot be used to address the conformation or the orientation of a specific residue.[25] For example, a 0º tilt angle of a membrane protein means that the protein lies parallel to the membrane whereas a 90º tilt angle shows that the protein forms a transmembrane structure. Therefore, 30.1 º which is the average tilt angle of the axis of all the thirty-five residues in α-syn(61-95) causes confusions about the behavior of α-syn(61-95) at the interface: will it be parallel to the interface or form transmembrane structure? There are two likely answers to this question as shown in **Figure 1.6**. One possibility is that the axis of all the thirty-five amino acid residues is 30.1 º as shown in **Figure 1.6A**. The other is that the axis of some residues is parallel whereas that of other residues are perpendicular as illustrated in **Figure 1.6B**.

The overall tilt angle of **Figure 1.6B** is also around 30.1 º. To address this issue, techniques with higher resolution (such as residue level resolution) result is needed.

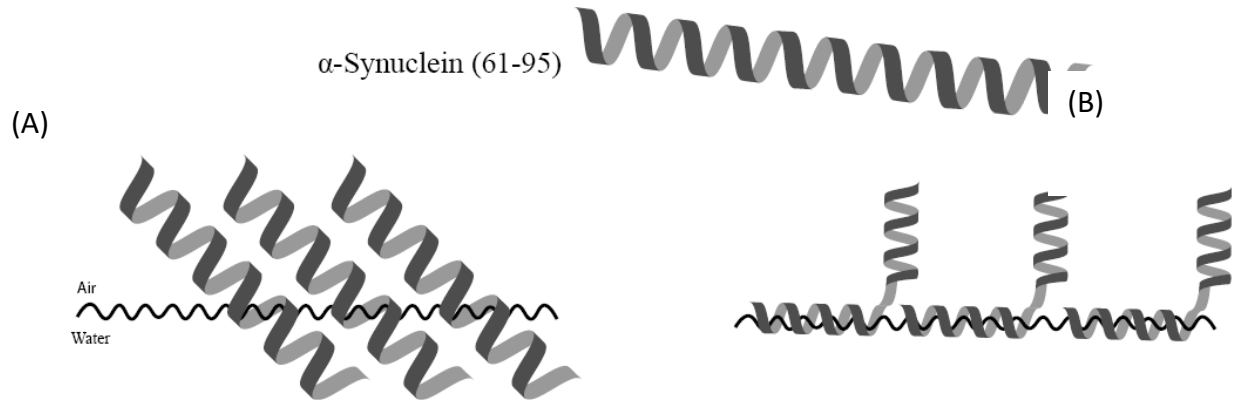

Figure 1.6. Illustration of two probabilities of α-syn(61-95) at the air-water interface.

Adapted from reference with permission[24]

Recently, the ^{13}C isotope-edited FT-IR spectroscopy was developed to provide residue level resolution by introducing ^{13}C isotopic labels into the backbone carbonyl (i.e., C=O) of a peptide/protein.[25, 35] The ^{13}C labeled C=O will generate a ^{13}C amide I band which can provide the conformation of a specific residue.[25, 36, 37]It was reported that biophysical behavior (such as conformation and orientation) of residues close to the terminus of might be different to the behavior of those in the middle of the sequence.[37] Therefore, ^{13}C isotopic label was introduced into the sequence of α-syn(61-95) in the backbone C=O of the glycine at position 93 (i.e., 93G), which is close to the C-terminus and serves as a proof-of-principle example by our research group. The pMAIRS results of the ^{13}C labeled α-syn(61-95) at 93G is shown in **Figure 1.7** below.

The in-plane spectrum (S_{IP}) of the ^{13}C labeled α-syn(61-95) is shown as the top curve in **Figure 1.7**. Like that of unlabeled α-syn(61-95) published before,[23] both regular amide I and II bands of α-helix were detected at 1655 and 1535 cm^{-1}, respectively. However, a very strong ^{13}C amide I band was also detected at 1625 cm^{-1} in the IP spectrum in **Figure 1.7**. The peak at 1625 cm^{-1} cannot be assigned to the β-sheets conformation because no signal of β-sheets was detected in the CD result. In addition, the ^{13}C amide I band in the IP spectrum is more intensive than the regular amide I band at 1655 cm^{-1}, which is the sum absorption of all the other thirty-four residues in the sequence of α-syn(61-95). As described in the selection rule in previous publication,[15] the peak intensity in pMAIRS can be affected by several factors such as thickness of the sample and the orientation of the transition moment. In the monolayer, the thickness of all the residues is almost the same and the orientation is the major factor to affect the peak intensity. Therefore, such an intensive ^{13}C amide I band suggests a very small tilt angle (i.e., parallel orientation) of the ^{13}C amide I transition moment.

The out-of-plane spectrum (S_{OP}), which is the bottom curve in **Figure 1.7** correlates to the IP spectrum and confirms this conclusion. The regular amide I and II bands were also detected in the S_{OP}. The regular amide I band splits slightly to 1659 and 1645 cm^{-1}, possibly stemming from the coupling between the regular and the ^{13}C amide I transition moment.[6] More importantly, the ^{13}C amide I band at 1625 cm^{-1} was very weak in the S_{OP} (i.e., the A_{OP} is almost zero for Equation 1 shown above), even though the ^{13}C label does exist at position 93G. According to the selection rule of pMAIRS shown in Equation 1 above, the tilt angle of the ^{13}C amide I transition moment at 93G is ~0º because the A_{OP} is almost zero. Consequently, the case shown in **Figure 1.6B** is the truth by the ^{13}C edited pMAIRS.

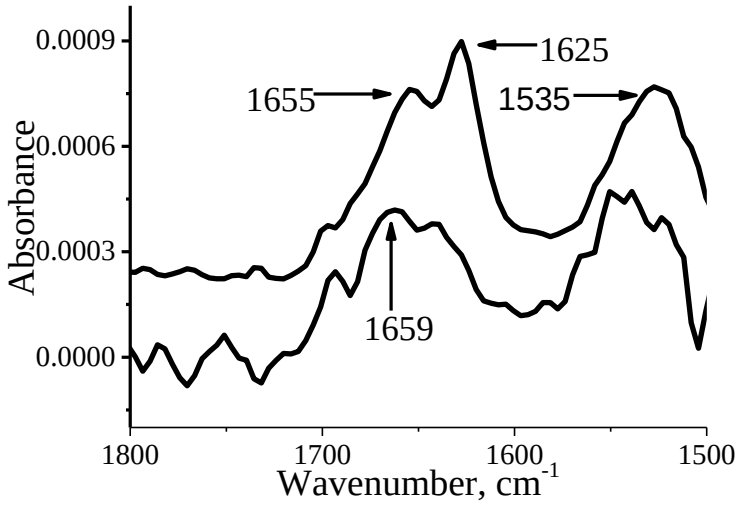

Figure 1.7. pMAIRS results of the LB monolayer of the ^{13}C labeled α-syn(61-95) at position 93G prepared at 10 mN/m on silicon slide. The top curve is the IP spectrum, and the bottom one is OP spectrum. Adapted from reference with permission[24]

1.7 Thesis Motivation.

The stability study of Langmuir monolayer of α-syn(61－95) is shown in **Figure 1.8**. The α-syn(61－95) Langmuir monolayer was compressed to a surface pressure of 6 mN/m and the surface pressure was kept constant over two hours. The surface pressure (solid line curve) and area (dashed line curve) were monitored over the entire experiment (*c.f.*, **Figure 1.8**). The area decreased similarly when the surface pressure increased from 0 to 6 mN/m, as shown in Figure 1.3.[23] After reaching 6 mN/m, the molecular area decreased more than 30 % within the first one hour. After that, the molecular area decreased only about 1% for the second hour of compression.

As discussed above,[23] α-syn(61－95) transformed to α-helix at the interface shortly (roughly after 15 minutes of compression) after it was spread by studying α-syn(61－95) monolayer by various spectroscopic techniques. Then, what happened during the two hours of compression that caused the significant decrease in the molecular area? From previous results (**Figure 1.5**), the tilt angle of the freshly prepared monolayer of α-syn(61－95) compressed at 6m/Nm was calculated to be 30.1º. Literature has shown that smaller proteins behave very similarly to small amphiphilic lipid molecules, which become more perpendicular to the interface when compressed[34]. This hypothesis provides insight into the rapid collapse in the area observed in the first hour of compression. We expect that after two hours of compression, the tilt angle will become more perpendicular to the interface and tilt angle should be greater than >30.1º.

To address the significant questions above, we introduced the ^{13}C label to the backbone carbonyl of first at position 93G in the C-terminus portion of the protein (α-syn(61－95)). This labeling allowed us to monitor the orientation with greater precision. The labeled protein was compressed for durations exceeding the initial 15 minutes, specifically extending the time to 2

hours and even 3 days. Despite the longer compression periods, we did not observe any significant differences in the orientation of the monolayer. The amide I transition moment at the residue was even more parallel to the interface as observed in the freshly prepared monolayer (15 minutes) compression (**Figure 1.7**). This was consistent with the previous observations made from the compression of the unlabeled protein (α-syn(61－95)).

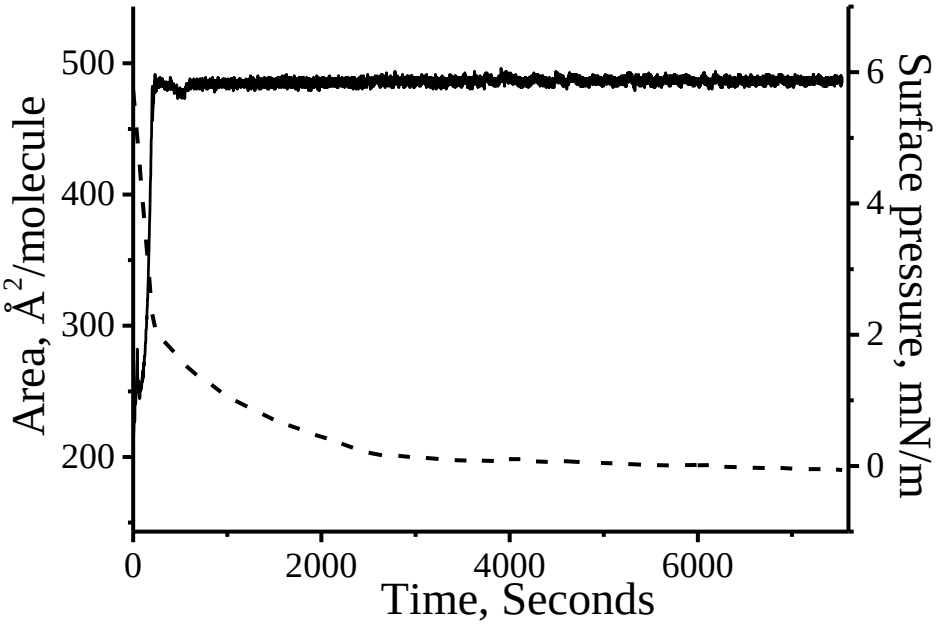

Figure 1.8. Stability curves when the Langmuir monolayer of α-syn(61－95) was compressed up to 6mN/m and kept constant for more than two hours on pure water subphase. The solid curve is for surface pressure, and the dashed curve is for the molecular area. Adapted from reference with permission[24]

In addition, α-syn is unstructured in an aqueous solution and transforms to α-helix in the presence of a membrane, we also know that α-syn aggregates to β-sheet conformation in Lewy Bodies. Is there any possibility of a conformation change of α-syn(61－95) during the compression? How about orientation? The pMAIRS result of isotope-labeled residue 93G did not provide any new information about a possible conformation change even after a longer duration of compression. This was also not in line with our earlier hypothesis to explain the sharp decline in the molecular area observed in **Figure 1.7**. Therefore, we decided to introduce ^{13}C isotope labeling at position 68G, which is in the N-terminus of the protein. The results further confirmed our knowledge of the possible conformation of the N-terminus portion of the protein, which we have shown to be tilted **(Figure 1.6B)**. A new hypothesis was proposed to explain the rapid reduction of the molecular area due to generating a new conformation and a more parallel residue orientation. All results are presented and discussed in Chapter 3.

CHAPTER 2

METHOD AND MATERIALS

2.1 Peptide Synthesis

The method of choice for the synthesis of all peptides used in this research was Solid Phase Peptide Synthesis (SPPS) using a CEM micro-wave peptide synthesizer (**Figure 2.1**). SPPS involves the buildup of amino acids from C-N terminal on an insoluble resin polymer support. The resin support used in our laboratory is a p-hydroxybenzyl alcohol linker attached to a polystyrene bead (Wang Resin). The polymer support was chosen due to easy cleavability even under mild acidic conditions along with its good swelling and mechanical properties.

The synthesis process is a continuous cycle of coupling-washing-deprotection-washing. The coupling process involves the reaction between C-terminus of the amino acid and the free amine group of the Wang Resin. The amine group of the free amino acid which is in DMF solution (*N,N*-dimethylformide) is protected by FMOC group (fluorenylmethyloxycarbonylchloride). The carboxylic group of the amino acid is activated for the coupling process by the addition of diisopropylcarbodiimide (DIC) and HOBt is added to suppress racemic products being formed.

The next step is to wash off the rest of the FMOC protected amino acids with DMF which is released, and the washing process is done a couple of times. After the solid support is washed, the FMOC protection on the amine of the amino acid coupled earlier is removed using a 1:4 mixture of piperidine and DMF. The washing process is repeated as we prepare the free amine for the next coupling sequence. This sequence is repeated until the desired target peptide is synthesized.

Figure 2.1. CEM microwave peptide synthesizer

The newly synthesized peptide is still attached to the solid polymer support (Wang resin). It would be cleaved firstly by the addition of DCM, followed by the suspension of the resin in a solution of 75% trifluoroacetic acid, 22% DCM, 1.5% triisopropylsilane, and 1.5% high purity water. The suspension was agitated to break the bond between the peptides C-terminal carboxylic group and the resin. Water and triisopropylsilane were utilized to scavenge both the t-butyl and tert-butoxycarbonyl protecting groups cleaved by the acid.

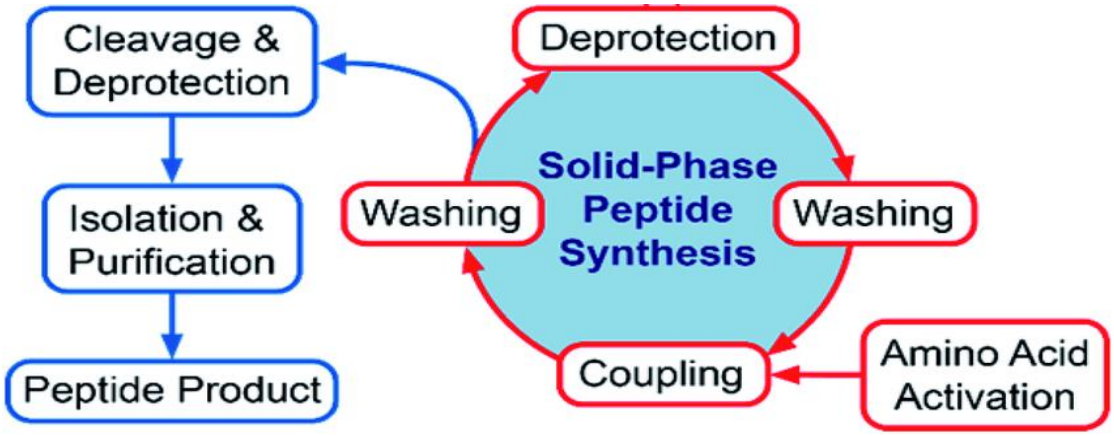

Figure 2.2. Overview of solid phase peptide synthesis

2.2 HPLC (High Performance Liquid Chromatography)

The crude sample (target peptide - α-syn (61–95)) is purified by HPLC using a solid support stationary phase (column) containing unmodified silica resins. Reverse phase chromatography is the method of choice for the peptide purification process. This involves a stationary phase which is an alkyl chain derivative such as the octadecyl group that is coupled onto the silica resins, adsorbing to hydrophobic molecules in the mobile phase. This makes it easier for the hydrophilic molecules to elute faster. The HPLC purification is performed with a Waters Breeze 2 separation system equipped with a 1525 EF binary pump and a column (Jupiter-10-C18-300, 10 mm i.d. × 250 mm) from Phenomenex (Torrance, CA) (**Figure 2.3**)

Figure 2.3. Waters Breeze 2 separation system

The mobile phases used were 0.1% trifluoroacetic acid in water (v/v, mobile phase A) and 0.1% trifluoroacetic acid in acetonitrile (v/v, mobile phase B). The elution gradient used 10-45% B for 40 min at a flow rate of 4.7 mL/min at 275 nm wavelength. The purified protein is stored as solid powder after lyophilization of the frozen sample kept at -80ºC.

2.3 Mass Spectroscopy

2.3.1 Mass Spectroscopy using Waters Synapt Tandem Mass spectrometer

The successfully synthesized peptide (α-syn (61–95)) is analyzed to confirm the molecular weight using an Electrospray ionization (ESI) equipped Time of Flight (TOF) mass spectrometer (Waters Synapt Tandem Mass spectrometer, Milford, MA) (**Figure 2.4**). The crude sample of the peptide was dissolved in DMSO and 0.5%TFA is nebulized from a small capillary to create an aerosol which is ionized by a coulombic charge of 3.00keV. The molecules of the ionized samples are accelerated towards the detector with the help of an electric field gradient.

Figure 2.4. Waters synaptic tandem mass spectrometer

A mass analyzer separates the accelerated molecular ion based on their mass to charge ratio. The sample procedure is used for the purified sample with a different solvent composition; in this case, high-purity water and 0.5% TFA are used. The temperature is kept at a constant 100ºC, and Nitrogen gas was used to keep the flow rate at 500L/hour.

2.3.2 Mass Spectroscopy Bruker Compact QTOF

Compact QTOF (Compass 1.9, otofControl 4.0) interfaced with electrospray ionization (ESI) Apollo source (Bruker Daltonics GmbH & Co. KG) (Figure 2.5) was also used to confirm successful synthesis. The synthesized peptide is injected through a column using 50% acetonitrile (ACN) (solvent A1) containing 0.1% formic acid (FA) (solvent B1). Positive-ion polarity mode was used at a spectrum rate of 4 Hz, Nitrogen gas supplied 0.6 bar was used to keep the dry temperature at 180oC, and the collision energy was kept at 7.0eV. Each collision energy data was acquired for 3 min in the range 100–2000 mz.

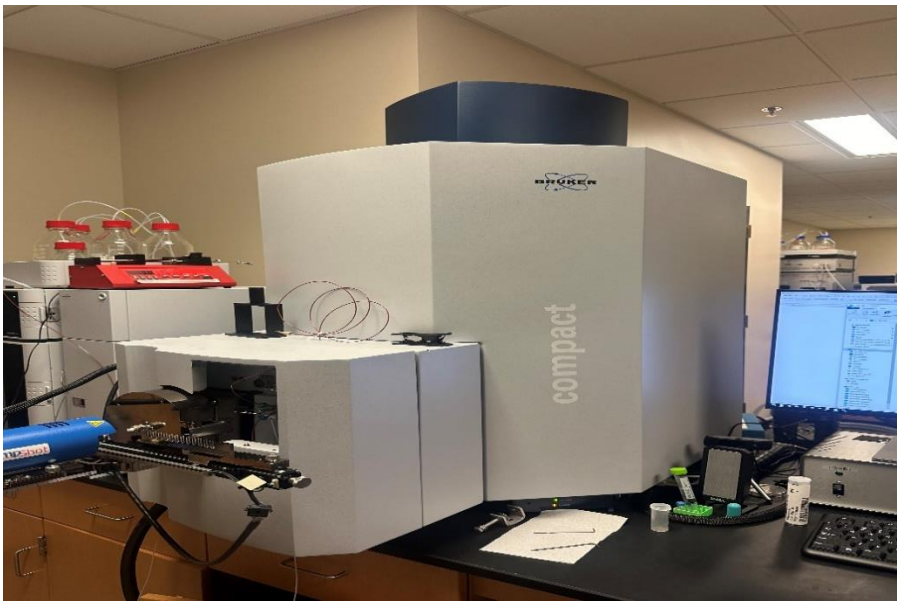

Figure 2.5 Compact QTOF (Compass 1.9, otofControl 4.0) interfaced with an electrospray ionization (ESI)

2.4 Langmuir Monolayer Technique.

The stability of the peptide (α-syn (61–95))was analyzed by measuring the surface pressure-area isotherm on pure water subphase.

Figure 2.6. Kibron μ-trough XS

The measurements were done by a Kibron μ-trough XS (Kibron Inc., Helsinki Finland) (**Figure 2.5**) under constant conditions of 20°C and 50% relative humidity. The purified sample is dissolved in water and at a concentration of 0.25mg/mL, and 25 μL is spread on the air-water interface in the trough. The monolayer is held at the interface by two barriers at a constant surface pressure of 6mN/m for varied time periods (15mins, 2hours and 4hours) after which it is transferred onto Si substrate at 0.3cm/minute.

2.5 p-Polarized Multiple Angle Incidence Resolution Spectroscopy (pMAIRS)

pMAIRS spectra is collected using a Thermo Fisher Scientific Nicolet 6700 iS50R FTIR equipped with Thermo Fischer Scientific (Waltham, MA, USA) pMAIRS accessory with a

mercury–cadmium–telluride detector cooled by liquid nitrogen (**Figure 2.6**). The monolayer of α-syn (61–95) was deposited on a bare Si substrate. A background spectrum is collected with the Si substrate prior to deposition of the monolayer, then another spectrum is collected with the sample deposited. Both 3000 and 9000 scans at 8cm^{-1} resolution were collected, and the in-plane (IP) and out-of-plane (OP) spectra were calculated based on the spectra collected.

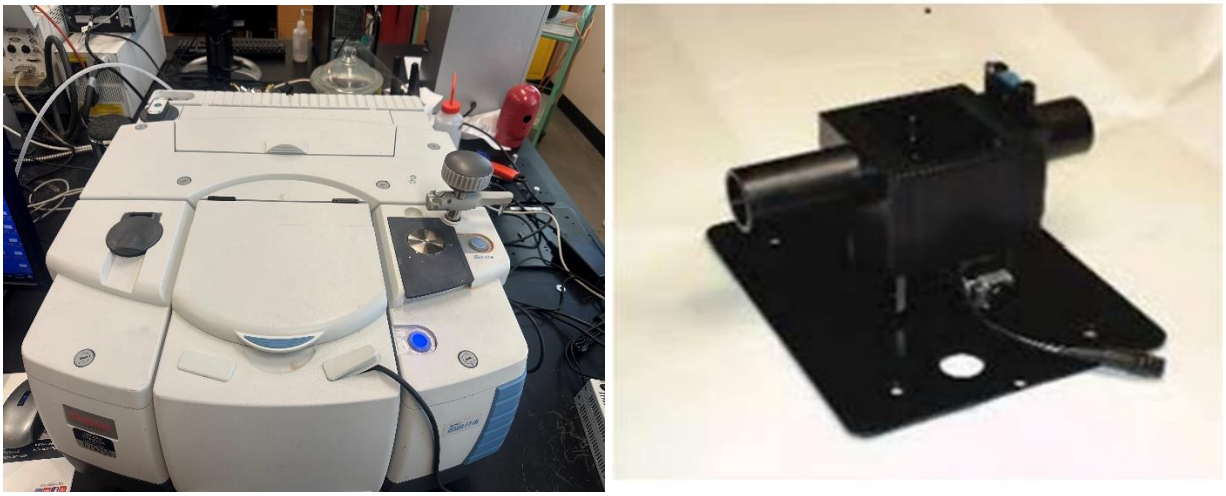

Figure 2.7. Thermo Fischer Nicolet iS50R FTIR with electronic rotary stage component

The orientation angle of the amide I band in relation to the surface normal was calculated with the equation (Equation 1.) discussed in the previous section. All results were repeated at least 3 times to confirm reproducibility.

CHAPTER 3

RESULTS AND DISCUSSIONS

3.1 Orientation May Cause the Decreasing Molecular Area.

It has been widely shown that compression usually caused the alkyl chains to become more perpendicular to the interface for small amphiphilic lipid molecules as shown in **Figure 3.1** below.[38, 39] To find out whether the axis of α-syn(61－95) in α-helix also becomes more perpendicular to the interface, unlabeled α-syn(61－95) was spread at the air-water interface again but compressed for two hours. Then, the monolayer of α-syn(61－95) was transferred onto Si substrate, which was measured by pMAIRS as shown in **Figure 3.2**.

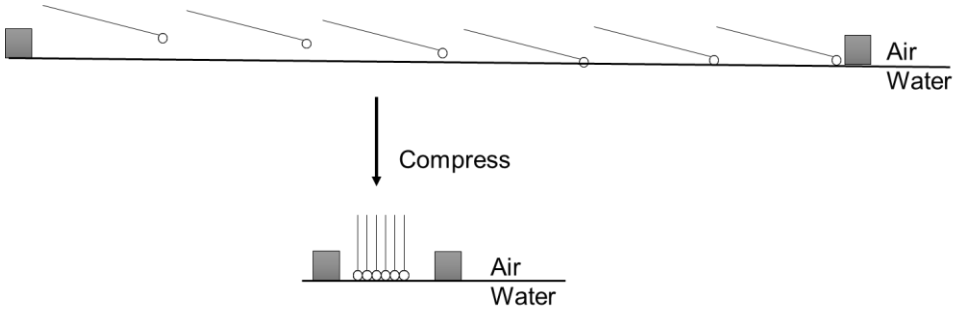

Figure 3.1. Illustration for small amphiphilic lipid molecules orient more perpendicular to the interface during the compression.

Figure 3.2 depicts the pMAIRS result containing S_{IP} and S_{OP} of the monolayer of unlabeled α-syn(61－95) transferred after two hours compression at 6 mN/m. As mentioned above, the pMAIRS results of the monolayer of unlabeled α-syn(61－95) transferred after compression at 6

mN/m for 15 minutes have been shown in **Figure 1.5**.[23] Similar to the **Figure 1.5**, the peak position of amide I band in both IP and OP spectra is at 1658 cm^{-1} which is the characteristic peak of α-helix. Therefore, α-helix is still the major conformation of α-syn(61－95) during the two hours compression. However, the intensity of the peak at 1658 cm^{-1} in S_{OP} result was lower than that transferred at 6 mN/m for 15 minutes as shown in **Figure 1.5**.[23]

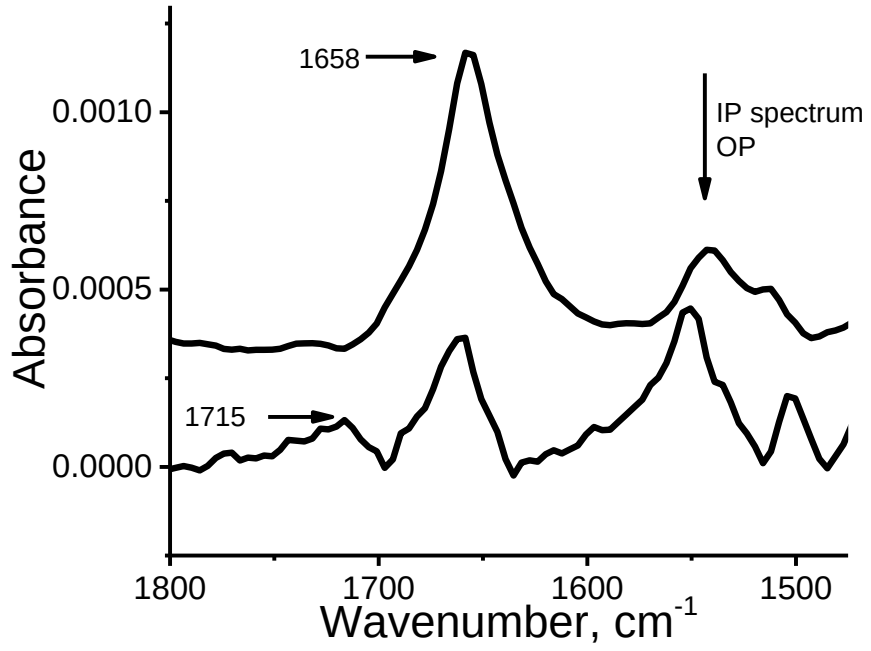

Figure 3.2. pMAIRS results of the LB monolayer of unlabeled α-syn(61－95) transferred after the surface pressure was held at 6 mN/m for two hours.

After calculation by the peak intensity at 1658 cm^{-1} according to Equation 1, the tilt angle of the amide I transition moment after two hours compression is 21.2º, also significantly lower than ~30.1 º calculated from **Figure 1.5**.[23] This difference in the tilt angle indicates that the reason of the fast decreasing in the surface area in **Figure 1.8** is the amide I transition moment of the α-helix becomes more parallel (not more perpendicular as shown in **Figure 3.1**). Two questions arise now: First, why more parallel orientation of α-helix decreases the molecular area? Second, what is the driving force to make the α-helical α-syn(61－95) more parallel to the interface, not more perpendicular?

As shown in **Figure 3.2** above, a peak at 1715 cm^{-1} was not detected in the IP result (the top curve in **Figure 3.2**) whereas detected in the OP result (the bottom curve in **Figure 3.2**). More interestingly, the peak at 1715 cm^{-1} was not detected in either the IP or the OP result for the monolayer of α-syn(61－95) transferred after 15 minutes compression as shown in **Figure 1.5**.[23] This peak indicates a probable subtle conformation change in some specific residues. To verify this hypothesis, ^{13}C label was introduced into the backbone carbonyl at position 68G and the ^{13}C labeled α-syn(61－95) will be spread at the interface. First, Mass spectroscopy was used to confirm the success of the synthesis and purification of the ^{13}C labeled α-syn(61－95) at 68G. The result from Waters q-TOF Mass spectrometer is shown in **Figure 3.3** below.

3.2 Mass Spectroscopy of ^{13}C Labeled α-Syn(61－95) at 68G

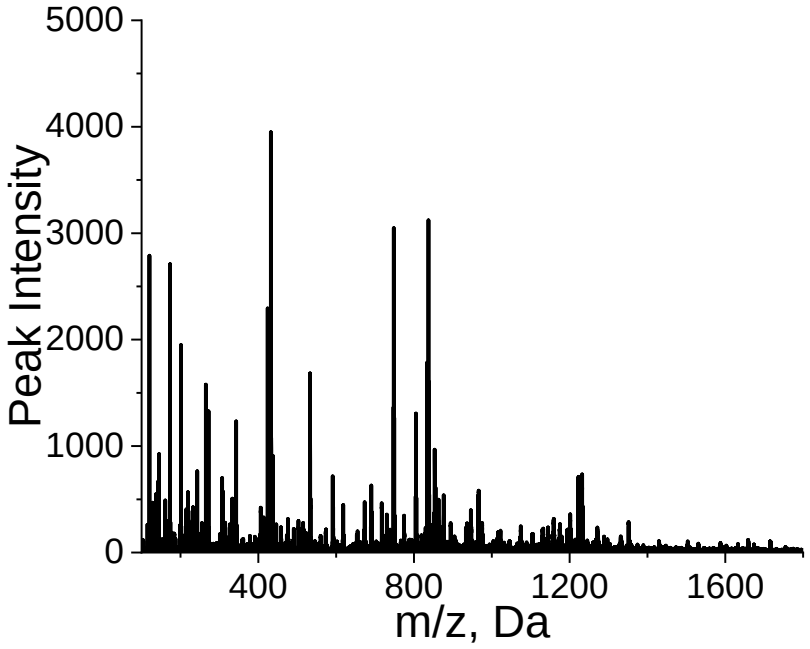

Figure 3.3. Mass spectroscopy from Waters q-TOF spectrometer.

The theoretical molecular weight of ^{13}C labeled α-syn(61－95) is 3302.8 Da and the doublet protonated ^{13}C labeled α-syn(61－95) should show a peak at 1652.4 Da. The ^{13}C labeled α-syn(61－95) with triple and four charges should show peaks at 1101.9 and 825.8 Da, respectively. All the peaks mentioned above did not show up in **Figure 3.3**. Thus, we tested the ^{13}C labeled α-syn(61－95) sample again by Bruker Mass spectrometer and the results are shown in **Figure 3.4** and **3.5**. Strong peaks were detected at 1652.44, 1101.59, and 825.03 Da in **Figure 3.4**. It must be mentioned that there are hundreds of carbon atoms in the ^{13}C labeled α-syn(61－95) molecule. The various isotopes of carbon, hydrogen, nitrogen, and oxygen may cause the molecular weight to vary. For example, the peak at 1652.44 Da in **Figure 3.4** was zoomed-in and the result is shown

in **Figure 3.5**. As shown in **Figure 3.5**, the molecular weight difference between the neighboring peak should be one but the charge of this peak is positive two. Consequently, the overall difference is the difference between any two neighboring peak is 0.5 Da, which is equal to one over two. After the confirmation of the success of the synthesis and purification, the ^{13}C labeled α-syn(61－95) was spread at the interface. Then the monolayer of ^{13}C labeled α-syn(61－95) transferred separately onto two Si substrates with the compression at 15 minutes and two hours, respectively. pMAIRS was used to compare the two monolayer samples and the results are shown below.

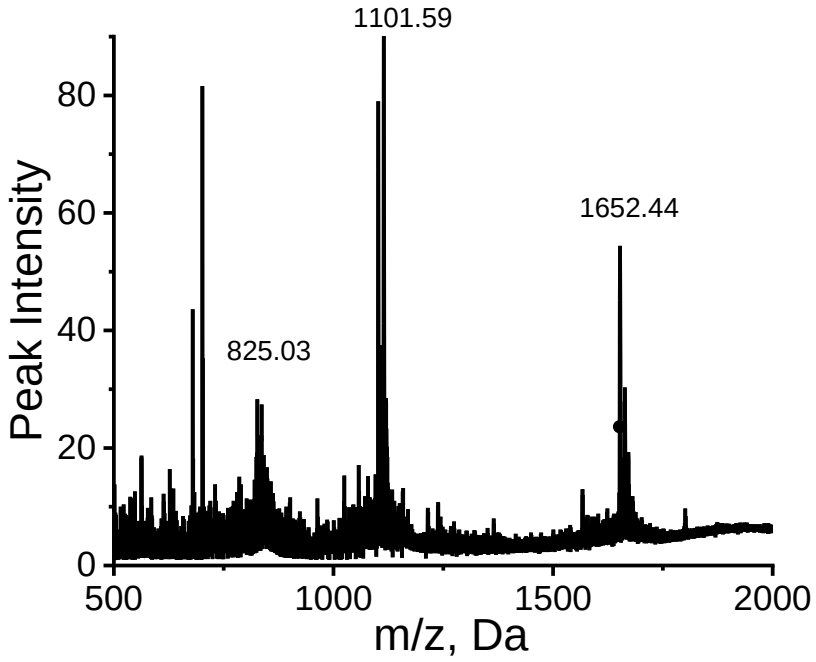

Figure 3.4. Mass spectroscopy from Bruker q-TOF spectrometer.

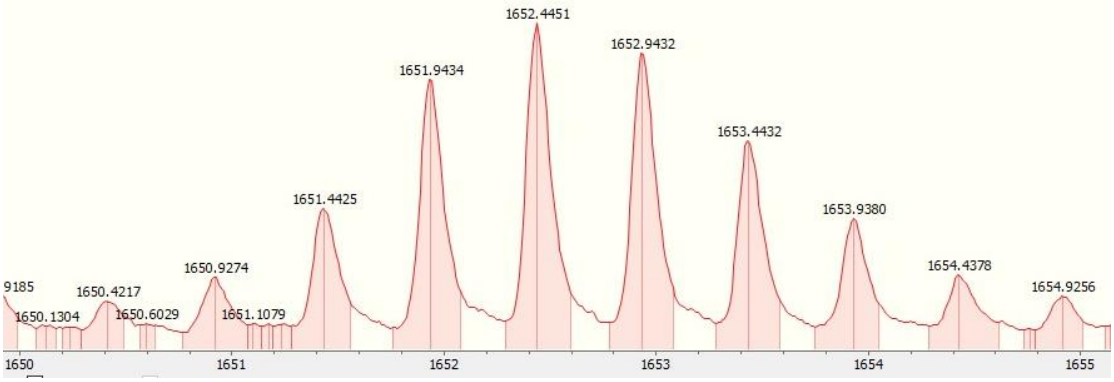

Figure 3.5. The zoom-in of the peak at 1652.44 Da.

3.3 Conformation Change was Detected by the pMAIRS of the Monolayer of ^{13}C Labeled α-syn(61－95) at 68G.

Figure 3.6 below depicts the pMAIRS results of the monolayer of ^{13}C labeled α-syn(61－95) at 68G transferred after compression for 15 minutes. In the IP result, which is the top curve in **Figure 3.6**, regular amide I and amide II band was detected at 1658 cm^{-1} and 1555 cm^{-1}, respectively. Although containing the ^{13}C label in the backbone, the ^{13}C labeled α-syn(61－95) does not show the ^{13}C amide I band around 1625 cm^{-1} clearly in the IP result as shown before.[23] Only a minor shoulder around 1625 cm^{-1} was detected and this is reasonable because only one ^{13}C label will not make the ^{13}C amide I band strong enough to show up when comparing the regular amide I band at 1658 cm^{-1}, which is the sum signal of all the other 34 residues. In the OP result (bottom curve of **Figure 3.6**), the regular amide I band also split at 1659 and 1645 cm^{-1} which are the same as published before for the unlabeled results.[23] The ^{13}C amide I band at 1625 cm^{-1} was detected in the OP result in **Figure 3.6**. Although suggesting a tilted (more perpendicular)

orientation, the ^{13}C amide I band in the OP result overlaps with the regular amide I band (detected at 1658 and 1645 cm^{-1}) which are similar to the result as previously published.[23] The overlapping peaks make it impossible to quantitatively calculate the tilted angle of the ^{13}C amide I transition moment by Equation 1 shown in the Introduction. Because **Figure 3.6** is the result of ^{13}C labeled α-syn(61－95) monolayer after compression for 15 minutes, the peak at 1715 cm^{-1} showing up in **Figure 3.2** (i.e., the pMAIRS result of unlabeled α-syn(61－95) monolayer transferred after compression for two hours) was not detected. As published before, the ^{13}C amide I band is about 15~30 cm^{-1} lower than its regular amide I band.[23] For example, the ^{13}C amide I band of α-helix was detected at 1625 cm^{-1} (*c.f.*, the OP curve in **Figure 3.6**) which is also ~30 cm^{-1} lower than the regular amide I band at 1658 cm^{-1} as shown in **Figure 3.6**.[23] Therefore, if there is any ^{13}C amide I band derives from the regular amide I band at 1715 cm^{-1} showing up in **Figure 3.2**, the position should be around 1685 cm^{-1}. But this peak was not detected in **Figure 3.6**, either. Consequently, we compressed the monolayer of ^{13}C labeled α-syn(61－95) for two hours and then transferred the monolayer to the substrate, which was examined by pMAIRS, and results are shown in **Figure 3.7**.

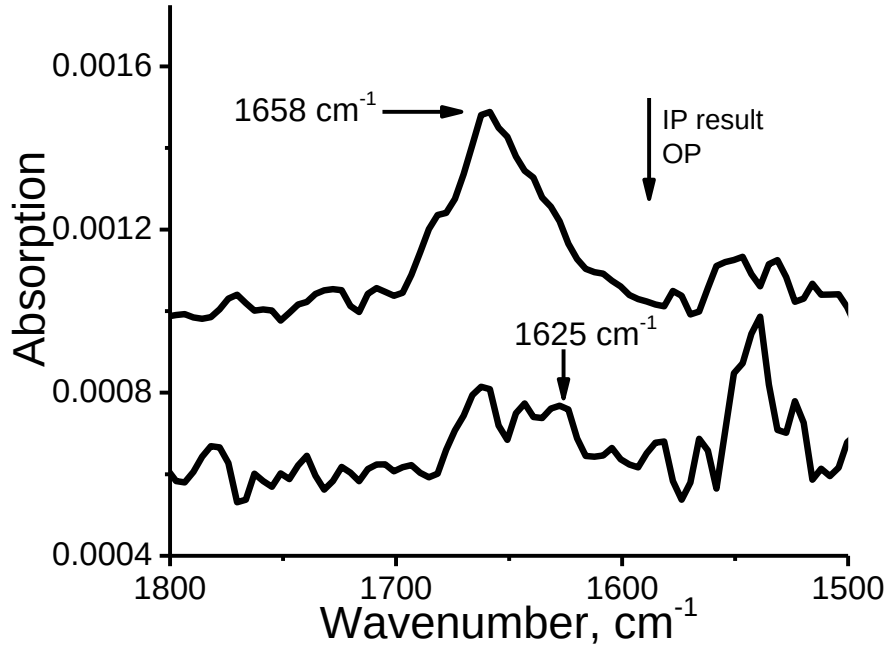

Figure 3.6. p-MAIRS results of the LB monolayer of ^{13}C labeled α-syn(61－95) at 68G transferred after the surface pressure was held at 6 mN/m for 15 minutes.

Compared with **Figure 3.6**, **Figure 3.7** shows the pMAIRS results from the monolayer of ^{13}C labeled α-syn(61－95) at 68G transferred after compression for two hours with similar IP result, which mainly detected the regular amide I band at 1658 cm^{-1}. Interestingly, a novel peak at 1685 cm^{-1} was detected in the OP result (the bottom curve in **Figure 3.7**) in addition to the regular and ^{13}C amide I band at 1658 and 1625 cm^{-1}, respectively. Furthermore, the novel peak at 1715 cm^{-1} detected in the OP result of **Figure 3.2** also appears in the OP result of **Figure 3.7**. Notice that both **Figures 3.2** and **3.7** are the pMAIRS results of the monolayer of α-syn(61－95) prepared under the same condition (i.e., transferred after compression of two hours). The only difference between

Figure 3.2 and **Figure 3.7** is that **Figure 3.7** shows the results of α-syn(61－95) with the single ^{13}C label at position 68G. Therefore, the peak at 1685 cm^{-1} in **Figure 3.7** is the ^{13}C amide I band from the regular amide I band at 1715 cm^{-1}. The novel peak at 1685 cm^{-1} is clear evidence that there is subtle conformation change specifically at 68G. Moreover, the peak at 1625 cm^{-1} was also detected as the ^{13}C amide I band of α-helix. Consequently, conformation change during the transition stage was detected.

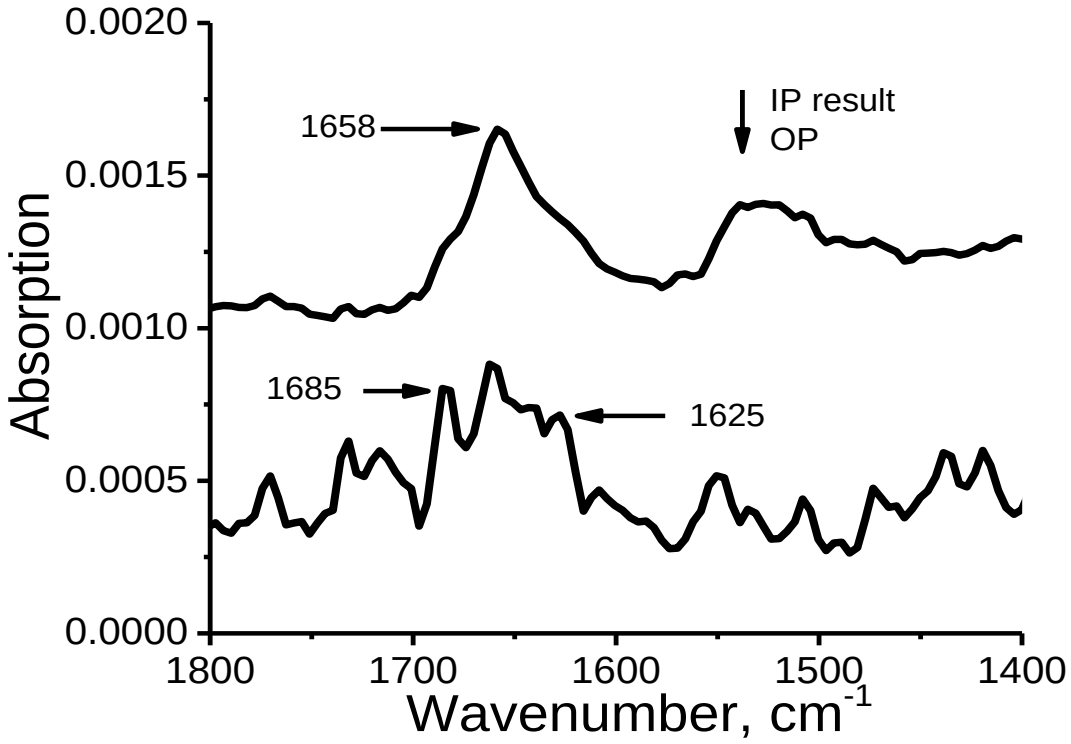

Figure 3.7. p-MAIRS results of the LB monolayer of ^{13}C labeled α-syn(61－95) at 68G transferred after the surface pressure was held at 6 mN/m for 2 hours.

It has been reported that the length of secondary structure can also affect the amide I band

position. For example, the long α-helix usually shows its amide I band around 1650 cm^{-1} whereas short α-helix may show it around 1658 cm^{-1}.[40,41] Because α-syn(61－95) only contains 35 residues, it is not a surprise that 1658 cm^{-1} was detected in **Figures 3.2**, **3.6**, and **3.7**. On the other hand, it has been widely accepted that anti-parallel β-sheet conformation shows its characteristic amide I bands at 1630 and 1695 cm^{-1}.[42] Although how the length affects the position of the amide I band of anti-parallel β-sheet conformation is still not very clear, we cannot rule out the probability that the peak at 1715 cm^{-1} stems from anti-parallel β-sheet conformation due to the short length of the peptide. To get more clear evidence of the formation of β-sheet conformation, the ^{13}C labeled α-syn(61－95) at 68G was compressed for longer time as shown below.

3.4 Results of Monolayer Compressed with Extensive Time

As shown in **Figure 3.8** below, a usual Langmuir monolayer trough can compress a monolayer for several hours. After that, water will evaporate substantially and even completely

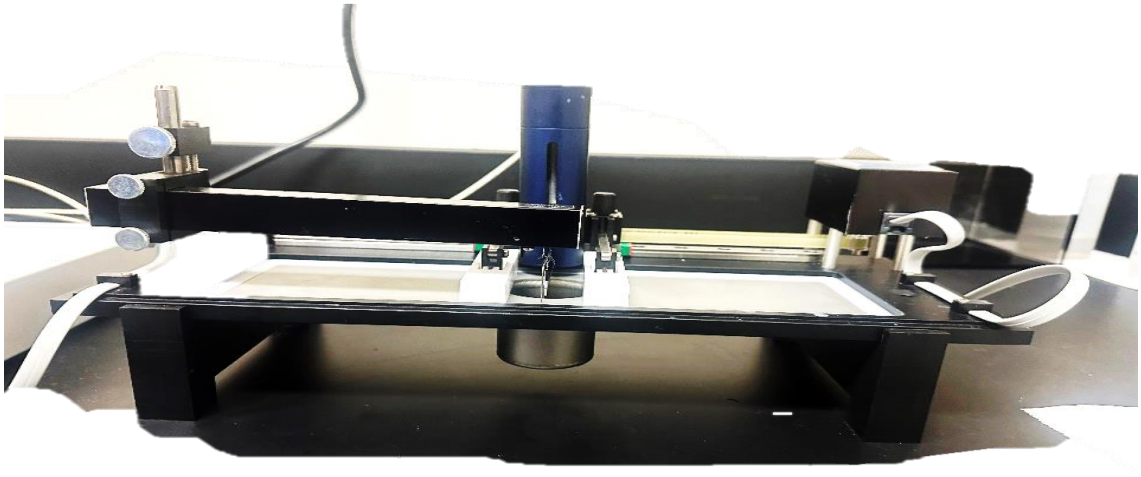

Figure 3.8. Usual Langmuir monolayer trough without the cover.

after 1 day in a lab with regular air conditioner. On the other hand, monolayers with two hours compression only show partial and even subtle conformation change as shown in **Figure 3.2** and **3.7**. To extend the compression time, we covered the trough and decreased the water evaporation as shown in **Figure 3.9** below. With the cover, monolayers can be compressed for 3 days with a stable surface pressure control. Then, the monolayer of ^{13}C labeled α-syn(61－95) at 68G was compressed for 3 days and the pMAIRS of the monolayer is shown in **Figure 3.10**.

Like **Figure 3.2** and **3.7**, the regular amide I band of α-helix was detected at 1658 cm^{-1} in the S_{IP} in **Figure 3.10**. A shoulder peak at 1632 cm^{-1} was also detected in the S_{IP} and this peak can be assigned to the regular β-sheet conformation. In addition, no ^{13}C amide I band was clearly detected in the S_{IP} in **Figure 3.10** due to the low abundance of ^{13}C label, because only one backbone carbonyl at 68G was ^{13}C labeled. As for S_{OP}, the shoulder peak at 1632 cm^{-1} was also detected and

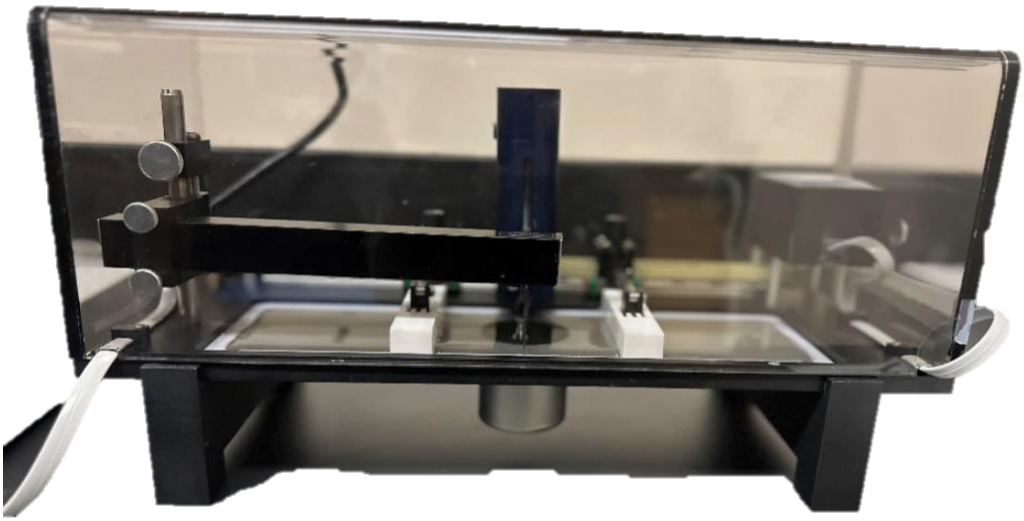

Figure 3.9. Langmuir monolayer trough with the cover

the peak at 1685 cm^{-1} was also detected. Most importantly, the ^{13}C amide I band was detected at 1616 cm^{-1} which is 16 cm^{-1} lower than that of the regular amide I band. Therefore, the peak at 1616 cm^{-1} is the ^{13}C amide I band of β-sheet conformation. Because only the backbone carbonyl at 68G was ^{13}C labeled, 68G changes its conformation from helix to β-sheet after three days compression.

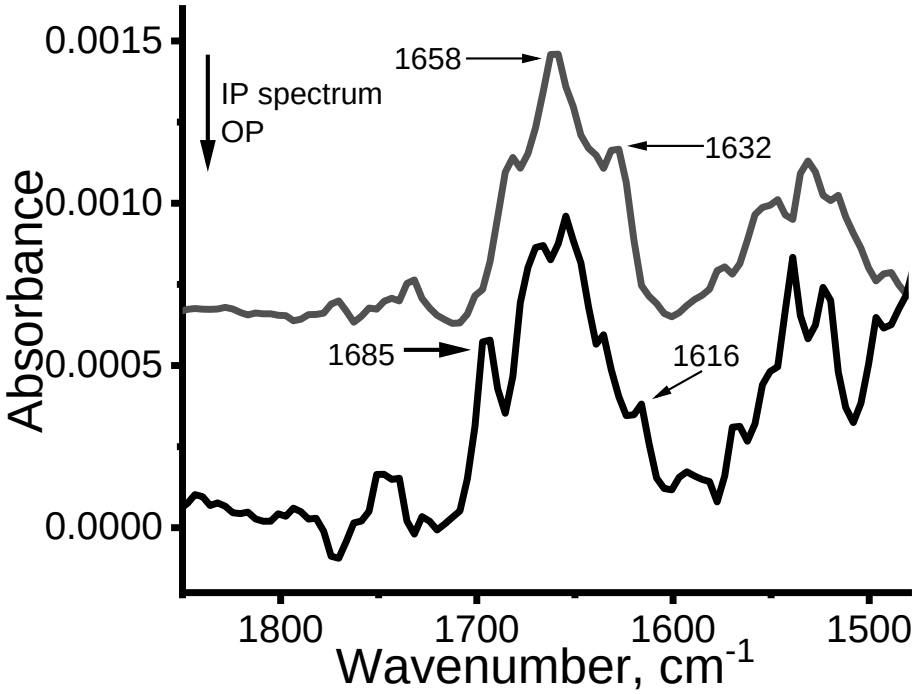

Figure 3.10. p-MAIRS results of the LB monolayer of ^{13}C labeled α-syn(61—95) at 68G transferred after the surface pressure was held at 6 mN/m for 3 days.

3.5 Discussions

It has been reported that α-syn(61－95) shows similar biophysical and biochemical behaviors to the α-syn whole protein.[23, 27] For example, both α-syn(61－95) and α-syn whole protein is unstructured in aqueous solution. When spread at the air-water interface, both of them transform to α-helix.[23, 27] On the other hand, the surface pressure-area isotherm of α-syn whole protein was stable during compression.[27] As shown in **Figure 1.8**, the area of α-syn(61－95) decreases substantially during the first hour of compression. Therefore, the N-terminus and the C-terminus of α-syn whole protein might make the α-syn more stable. In other words, the N-terminus (residue 1-60) and C-terminus (95-140) of α-syn whole protein may inhibit the potential conformation change in the presence of amphiphilic natures around the presynaptic terminals.

According to the selection rules of pMAIRS, the tilted angle of both conformations can be evaluated specifically for 68G. However, 1625 cm^{-1} overlap substantially with the regular amide I band at 1658 cm^{-1}, especially showing as a shoulder peak in the IP results shown in both **Figure 3.6** and **3.7**. The overlap makes it difficult to quantitatively determine the axis of remaining α-helical conformation at 68G. This issue can be addressed by simultaneously introducing ^{18}O isotope together with ^{13}C into the backbone carbonyl. The $^{13}C=^{18}O$ has been reported to downshift the amide I band to 1595 cm^{-1},[6] which separates well from the regular amide I band of α-helix. Similarly, the ^{13}C amide I band for β-sheet conformation may also be moved to ~1600 cm^{-1}. On the other hand, the potential labeling of ^{18}O may also downshift the novel peak at 1685 cm^{-1} in the OP result in **Figure 3.7** and **3.10** to ~1655 cm^{-1}, which also overlaps the regular amide I band of α-helix. Therefore, duplicate labeling by various isotopes at the same position will be still important to quantitatively evaluate the tilted angle of the newly generated conformation at 68G.

Furthermore, both 1685 cm^{-1} and 1625 cm^{-1} were detected in the OP result shown in **Figure**

3.7. Because its absence in the IP result (the top curve) in **Figure 3.7**, the novel peak at 1685 cm^{-1} showed the very perpendicular orientation for the amide I transition moment at 68G. Interestingly, the ^{13}C amide I band at 1625 cm^{-1} was also detected in OP results (the bottom curve) of both **Figure 3.6** and **3.7**. The ^{13}C amide I band at 1625 cm^{-1} in **Figure 3.7** stems from the remaining α-helical conformation in 68G. As previously published,[23] the axis of the α-helix is roughly parallel to the amide I transition moment. Consequently, the ^{13}C amide I band at 1625 cm^{-1} only shows as a shoulder peak in the IP result (the top curve) in **Figure 3.6** suggests that the axis of α-helix at 68G or even the N-terminus is tilted to the interface as shown in **Figure 3.11** below before the compression. On the other hand, our previous publication that the C-terminus is parallel to the interface by introducing ^{13}C label at the backbone carbonyl of 93G as illustrated in **Figure 1.6**.[24] The tilted orientation of N-terminus may facilitate the conformation change, which may result in the formation of intermolecular hydrogen bond in the N-terminus and decrease the molecular area with compression as shown in **Figure 1.8**. Thus, the more tilted orientation of N-terminus of α-syn(61－95) facilitates the conformation change whereas the parallel C-terminus remains in α-helix as shown in **Figure 3.11** after compression. We also compressed the monolayer of ^{13}C labeled α-syn(61－95) at 93G for more than two days and analyzed it by pMAIRS. However, no conformation change was detected (results not shown). Therefore, subtle conformation change occurs in the N-terminus around residue 68G which results in the overall orientation of α-helix more parallel (from 32.2 ° to 21.2 º) as detected in **Figure 3.2** and illustrated by **Figure 3.11** below.

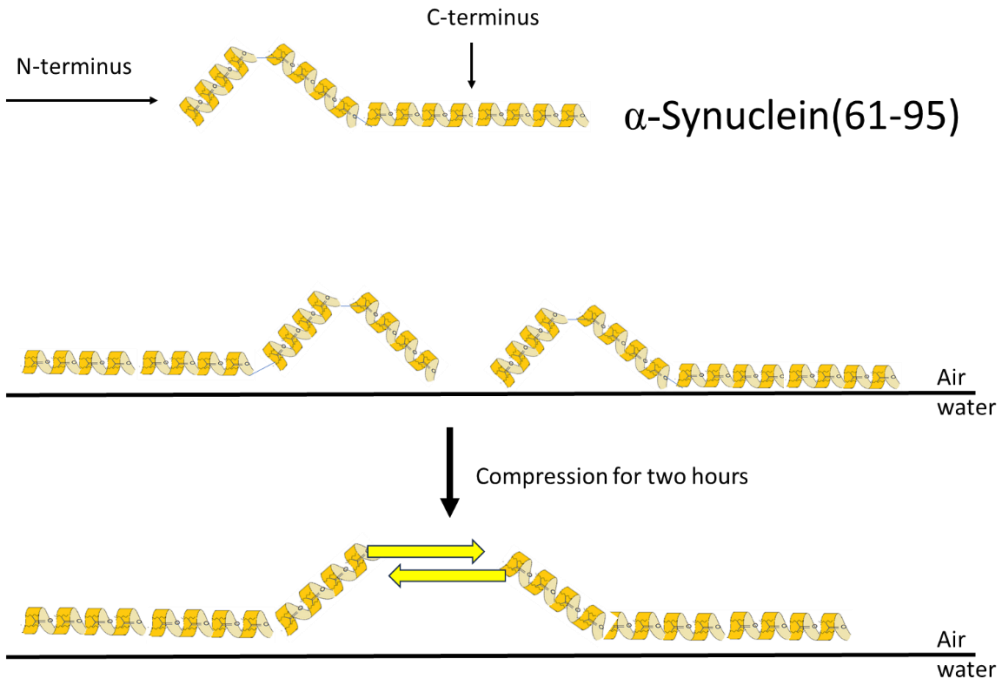

Figure 3.11. Conformation changes with intermolecular hydrogen bond formation during the compression of α-syn(61－95) at interface.

Finally, spontaneous detection of the peaks at 1685 and 1625 cm^{-1} mentioned above definitely shows that the partial conformation change occurs specifically at residue 68G. If α-helix completely changes to other conformation at 68G, the peak at 1625 cm^{-1} from α-helix would disappear in the OP result (the bottom curve) of **Figure 3.7**. In other words, the transition during the conformation change of α-syn(61－95) was snapshot in a specific residue even in monolayer by pMAIRS. This accomplishment means pMAIRS can supplement other techniques to address protein's structure as mentioned in the Introduction. Coexisting conformation occurring in a specific residue may cause challenges for the three major techniques (i.e., X-ray, NMR, and Cryo-EM) to provide high resolution results. For example, Cryo-stat EM has also been utilized to

analyze the aggregates structure of α-synuclein whole protein. During the aggregation, two conformations often equilibrates in some residues and this equilibrium substantially challenges the resolution of cryo-stat EM.[43-45] Therefore, pMAIRS may supplement the techniques above to help to address the structure of α-syn whole protein (or even other amyloidogenic proteins) in various aggregation stages.

3.6 Conclusion

The monolayer formed by α-syn(61－95) at the interface was compressed at various times and transferred to solid substrate for pMAIRS analysis. After compression for two hours, a novel conformation was detected by pMAIRS in the monolayer of unlabeled α-syn(61－95) due to the generation of a new peak at 1715 cm^{-1} which only appears in the OP result. Single ^{13}C isotope label was introduced into the backbone carbonyl of α-syn(61－95) at 68G and monolayer of the ^{13}C labeled α-syn(61－95) was also analyzed by pMAIRS. After 15 minutes compression, the ^{13}C label only showed up the ^{13}C amide I band at 1625 cm^{-1} (assigned to α-helix) in the OP result. On the other hand, two ^{13}C amide I band at 1685 cm^{-1} and 1625 cm^{-1} were detected simultaneously in the OP result of pMAIRS after compression for two hours.

The peak at 1685 cm^{-1} which is 15~30 cm^{-1} lower than that at 1715 cm^{-1} was assigned to another conformation. Therefore, coexisting conformation (i.e., the transition stage during the conformation change) at specific 68G residue was detected by pMAIRS even in monolayer. This clearly shows that pMAIRS can supplement other techniques to provide high resolution results for membrane protein's structure. After three days compression, the ^{13}C amide I band in the pMAIRS result of ^{13}C labeled α-syn(61－95) at 68G moved to 1616 cm^{-1}, which is assigned to β-sheet conformation. This downshift confirms the conformation change at 68G.

CHAPTER 4

REFERENCES

1. M. Chen, M. Margittai, J. Chen and R. Langen, J. Biol. Chem. 282, 24970-24979 (2007).
2. H. Heise, W. Hoyer, S. Becker, O. C. Andronesi, D. Riedel and M. Baldus, Proc. Nat. Acad. Sci. U.S.A. 102 (15871-15876) (2005).
3. W. H. Massover, J. Synchrotron Radiat. 14, 116-127 (2007).
4. Y. Cheng, Curr. Opin. Struct. Biol. 52, 58-63 (2018).
5. A. Krogh, B. Larsson, G. Heijne and E. L. L. Sonnhammer, J. Struct. Biol. 305, 567-580 (2001).
6. J. Manor, E. Arbely, A. Beerlink, M. Akkawi and I. T. Arkin, J. PHys. Chem. Lett. 5, 2573-2579 (2014).
7. X. Yao, X. Fan and N. Yan, Proc. Nat. Acad. Sci. U.S.A. 117, 18497-18503 (2020).
8. C. G. Dudzik, E. D. Walter, B. S. Abrams, M. S. Jurica and G. L. Millhauser, Biochemistry 52, 53-60 (2013).
9. R. Kahn, P. Carpentier, C. Berthet-Colominas, M. Capitan, M. L. Chesne, E. Fanchon, S. Lequien, D. Thiaudiere, J. Z. Vicat, P. and H. Stuhrmann, J. Synchront. Rad. 7, 131-138 (2000).
10. J. K. Lanyi, Mol. Membrane Biol. 21, 143-150 (2004).
11. Y. Xu and S. Dang, Front. Mol. Biosci. 9, 892459 (2022).
12. L. Zhou and D. Kurouski, Anal. Chem. 92, 6806-6810 (2020).
13. R. M. Fabre, G. O. Okeyo and D. R. Talham, Langmuir 28, 2835-2841 (2012).
14. R. M. Nyffenegger and R. M. Penner, Chem. Rev. 97, 1195-1230 (1997).
15. T. Hasegawa, *Quantitative Infrared spectroscopy for understanding of a condensed matter*. (Springer 2017).
16. O. Teschke and E. F. de Souza, Langmuir 18, 6513-6520 (2002).
17. O. Teschke and E. F. de Souza, Chem. Phys. Lett. 403, 95-101 (2005).
18. L. Dziri, B. Desbat and R. M. Leblanc, J. Am. Chem. Soc. 121, 9618-9625 (1999).
19. G. Yang, Y. Dong, K. Gong, W. Jiang, E. Kwon, P. Wang, H. Zheng, X. Zhang, W. Gan and N. Zhao, Neurosci. Lett. 384, 66-71 (2005).

20. R. M. Fabre and D. R. Talham, Langmuir 25, 12644-12652 (2009).

21. X. Du, W. Miao and Y. Liang, J. Phys. Chem. B 109, 7428-7434 (2005).

22. T. Hasegawa, J. Nishijo, M. Watanabe, J. Umemura, Y. Ma, G. Sui, Q. Huo and R. M. Leblanc, Langmuir (12), 4758-4764 (2002).

23. C. Wang, S. K. Sharma, S. O. Olaluwoye, S. A. Alrashdi, T. Hasegawa and R. M. Leblanc, Colloid. Surf. B 183, 110401 (2019).

24. C. Wang, Y. Zhou, C. Ewuola, T. Akinleye, T. Hasegawa and R. M. Leblanc, Anal. Sci. 38, 935-940 (2022).

25. S. M. Decatur, Acc. Chem. Res. 39, 169-175 (2006).

26. E. Maltseva, A. Kerth, A. Blume, H. Mohwald and G. Brezesinski, Chembiochem 6, 1817-1824 (2005).

27. C. Wang, N. Shah, G. Thakur, F. Zhou and R. M. Leblanc, Chem. Commun. 46, 6702-6704 (2010).

28. M. G. Spillantini, R. A. Crowther, R. Jakes, M. Hasegawa and M. Goedert, Proc. Natl. Acad. Sci. U. S. A. 95, 6469-6473 (1998).

29. M. G. Spillantini, M. L. Schmidt, V. M. Y. Lee, J. Q. Trojanowski, R. Jakes and M. Goedert, Nature 388, 839-840 (1997).

30. K. Beyer, Acta Neuropathol. 112, 237–251 (2006).

31. Z. Qin, D. Hu, S. Han, D. Hong and A. L. Fink, Biochemistry 46, 13322-13330 (2007).

32. L. Breydo, J. W. Wu and V. N. Uversky, Biochim. Biophys. Acta. 1822, 261-285 (2012).

33. H. Han, P. H. Weinreb and P. T. Lansbury, Chem. Biol. 2, 163-169 (1995).

34. A. L. Fink, Acc. Chem. Res. 39, 628-634 (2006).

35. S. A. Petty and S. M. Decatur, J. Am. Chem. Soc. 127, 13488-13489 (2005).

36. S. Li, J. D. Combs, O. E. Alharbi, J. Kong, C. Wang and R. M. Leblanc, Chem. Commun. 51, 12537-12539 (2015).

37. S. Li, P. Sneha, J. D. Keith, C. Wang and R. M. Leblanc, Chem. Commun. 50, 3931-3933 (2014).

38. C. Wang, C. Li, X. Ji, J. Orbulescu, J. Xu and R. M. Leblanc, Langmuir 22, 2200-2204 (2006).

39. C. Wang, J. Zheng, O. N. Oliveira and R. M. Leblanc, J. Phys. Chem. C 111, 7826-7833 (2007).

40. L. Pauling and R. B. Corey, Proc. Nat. Acad. Sci. U.S.A. 37, 729-740 (1951).

41. E. Goormaghtigh, V. Cabiaux and J. M. Ruysschaert, Subcell. Biochem. 23, 329-450 (1994).

42. N. Demirdoven, C. M. Cheatum, H. S. Chung, M. Khalil, J. Knoester and A. Tokmakoff, J. Am. Chem. Soc. 126, 7981-7990 (2004).

43. S. W. Chen, S. Drakulic, E. Deas, M. Ouberai, F. A. Aprile, R. Arranz, S. Ness, C. Roodveldt, T. Guilliams, E. J. De-Genst, D. Klenerman, N. W. Wood, T. P. J. Knowles, C. Alfonso, G. Rivas, A. Y. Abramov, J. M. Valpuesta, C. M. Dobson and N. Cremades, Proc. Nat. Acad. Sci. U.S.A. 112, E1994-E2003 (2015).

44. N. Lorenzen, S. B. Nielsen, A. K. Buell, J. D. Kaspersen, P. Arosio, B. S. Vad, W. Paslawski, C. G., Z. Valnickova-Hansen, M. Andreasen, J. J. Enghild, J. S. Pedersen, C. M. Dobson, T. P. J. Knowles and D. E. Otzen, J. Am. Chem. Soc. 136, 3859-3868 (2014).

45. W. Paslawski, S. Mysling, K. Thomsen, T. J. D. Jorgensen and D. E. Otzen, Angew. Chem. Int. Ed. 53, 7560-7563 (2014).